BOLETÍN DE LA SOCIEDAD ESPAÑOLA DE CERÁMICA Y VIDRIO XXX (2016) XXX–XXX

BOLETIN DE LA SOCIEDAD ESPAÑOLA DE
Cerámica y Vidrio
www.elsevier.es/bsecv

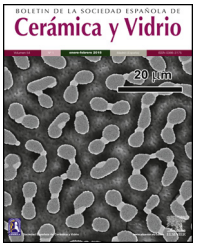

Control of the γ-alumina to α-alumina phase transformation for an optimized alumina densification

Samir Lamouri[a,*], *Mohamed Hamidouche*[b], *Noureddine Bouaouadja*[a], *Houcine Belhouchet*[a,c], *Vincent Garnier*[d], *Gilbert Fantozzi*[d], *Jean François Trelkat*[e]

[a] *Non-Metallic Materials Laboratory, Optics and Precision Mechanics Institute, Ferhat Abbas University Setif 1, Setif, Algeria*
[b] *Emerging Materials Research Unit, Ferhat Abbas University Setif 1, Setif, Algeria*
[c] *Physics Department, Faculty of Sciences, University Mohamed Boudiaf of M'sila, M'sila, Algeria*
[d] *Laboratory MATEIS (UMR CNRS 5510), Bat. Blaise PASCAL, INSA Villeurbanne, Villeurbanne, Lyon, France*
[e] *Valenciennes University, LMCPA Boulevard Général de Gaulle, Maubeuge, France*

ARTICLE INFO

Article history:
Received 26 May 2016
Accepted 17 October 2016
Available online xxx

Keywords:
Transition alumina
Phase transformation
Densification
Microstructure

ABSTRACT

In this work, we studied the aptitude to sintering green bodies using γ-Al_2O_3 transition alumina as raw powder. We focused on the influence of the heating rate on densification and microstructural evolution. Phase transformations from transition alumina γ → δ → θ → α-Al_2O_3 were studied by in situ X-rays diffraction from the ambient to 1200 °C. XRD patterns revealed coexistence of various phase transformations during the heating cycle. DTA and dilatometry results showed that low heating rate leads to a significant reduction of the temperature of the α-Al_2O_3 alumina formation. Around 1190, 1217 and 1240 °C were found when using 5, 10 and 20 °C/min of heating rate, respectively. The activation energy for θ-Al_2O_3 → α-Al_2O_3 transformation calculated by Kissinger and JMA equations using dilatometry method were 464.29 and 488.79 kJ/mol, respectively and by DTA method were 450.72 and 475.49 kJ/mol, respectively. In addition, the sintering of the green bodies with low heating rate promotes the rearrangement of the grains during θ-Al_2O_3 → α-Al_2O_3 transformation, enhancing the relative density to 95% and preventing the development of a vermicular structure.

© 2016 SECV. Published by Elsevier España, S.L.U. This is an open access article under the CC BY-NC-ND license (http://creativecommons.org/licenses/by-nc-nd/4.0/).

Control de la transformación de fase gamma-alúmina a α-alúmina para una densificación óptima

Palabras clave:
Alúmina de transición
Transformación de fase
Densificación
Microestructura

RESUMEN

En este trabajo, se ha estudiado la capacidad de sinterización de muestras en verde a partir de γ-Al_2O_3 de transición en forma de polvo. El trabajo se ha focalizado en la influencia de la velocidad de calentamiento sobre la densificación y la evolución microestructural. Las transformaciones de fase de alúminas de transición γ→δ→θ→α-Al_2O_3 se han estudiado in situ mediante Difracción de Rayos X (DRX) desde temperatura ambiente hasta 1.200 °C.

* *Corresponding author.*
E-mail address: samirlamouri@univ-setif.dz (S. Lamouri).
http://dx.doi.org/10.1016/j.bsecv.2016.10.001
0366-3175/© 2016 SECV. Published by Elsevier España, S.L.U. This is an open access article under the CC BY-NC-ND license (http://creativecommons.org/licenses/by-nc-nd/4.0/).

Please cite this article in press as: S. Lamouri, et al., Control of the γ-alumina to α-alumina phase transformation for an optimized alumina densification, Bol. Soc. Esp. Cerám. Vidr. (2016), http://dx.doi.org/10.1016/j.bsecv.2016.10.001

Los diagramas de XRD han revelado la coexistencia de diversas transformaciones de fase durante el ciclo de calentamiento. Los Análisis Térmicos Diferenciales (ATD) realizados y los datos de dilatometría han mostrado que velocidades de calentamiento bajas conducen a una reducción significativa de la temperatura de formación de α-Al_2O_3. Detectándose alrededor de 1.190, 1.217 y 1.240 °C cuando se utilizan 5, 10 y 20 °C/min como velocidad de calentamiento, respectivamente. La Energía de Activación para la transformación θ-$Al_2O_3 \rightarrow \alpha$-$Al_2O_3$ calculada mediante las ecuaciones de Kissinger y JMA usando métodos dilatometricos han sido 464,29 y 488,79 kJ/mol, respectivamente, y mediante ATD 450,72 y 475,49 kJ/mol, respectivamente. Además, la sinterización con velocidad de calentamiento baja promueve la reorganización de los granos durante la transformación θ-$Al_2O_3 \rightarrow \alpha$-$Al_2O_3$, el aumento de la densidad relativa al 95% y la prevención del desarrollo de una estructura vermicular.

© 2016 SECV. Publicado por Elsevier España, S.L.U. Este es un artículo Open Access bajo la licencia CC BY-NC-ND (http://creativecommons.org/licenses/by-nc-nd/4.0/).

Introduction

Due to its interesting physico-chemical and mechanical properties, alumina is one of the most used technical ceramics as structure parts, applied in medical use (orthopaedic implants) and electronics [1–5]. To obtain dense alumina products, a perfect processing control from powder synthesis to sintering [6,7] is required. Gibbsite ($Al(OH)_3$) and boehmite (AlOOH) are the most used precursors for the preparation of α-Al_2O_3. During the heat treatment, aluminium hydroxides transform into transition alumina in the form of metastable structure before ending as α-Al_2O_3 thermodynamic stable phase (Fig. 1) [8,9]. Boehmite transforms into γ-Al_2O_3 transition alumina under a temperature range of 500–550 °C with a departure of structural water [10]. The transformation of γ-Al_2O_3 monoclinic phase ($d = 3.56\,g\,cm^{-3}$) to α-Al_2O_3 hexagonal phase ($d = 3.98\,g\,cm^{-3}$) is accompanied by a volume reduction of about 10% causing a large density increase [11–14]. The transformation of θ-Al_2O_3 transition alumina to α-Al_2O_3 takes place in the temperature range 1050–1200 °C. This transformation occurs through a nucleation and grains growth mechanism [15–18] and is influenced by several parameters such as grain size [19], chemical composition [20] and heating rate [21]. The θ-$Al_2O_3 \rightarrow \alpha$-$Al_2O_3$ transformation is very significant for the sintering process and consequently for the control of microstructure [22]. According to the sintering conditions, the formation of crystalline α-Al_2O_3 can produce a vermicular microstructure form consisting of a wide pores network, which develops during the α-Al_2O_3 transformation [23,24]. In addition, it is difficult to study with precision the transformation of transition alumina phases due to their instability and high reactivity [21]. Different studies showed that a high energy milling influences the phase transformation from transition alumina to α-Al_2O_3 stable phase [25–29]. Specific diagrams defining the pathway of phase transformations were established according to the heating temperature and particle grain size [10,30]. Some studies were conducted using coarse and fine grained gibbsite in order to examine the transformation paths using in situ X-rays diffraction [19]. Others concern the gibbsite and boehmite to α-Al_2O_3 phase transformation cases. They noticed that small α-Al_2O_3 crystallites of spherical form are obtained by boehmite transformation and larger ones in plate form from gibbsite [31]. The raw powder and the milling mode are therefore fundamentally important for the sintering process and the densification. Many techniques are used to improve the densification process like α-Al_2O_3 seeds [32,33] and the alumina doping agents [34].

In this work we used γ-Al_2O_3 transition alumina as raw powder to study the densification process and the microstructure of sintered samples using various heating rates. The γ-Al_2O_3 to α-Al_2O_3 transformation was characterized in situ by XRD, and the activation energy accompanying the θ-Al_2O_3 to α-Al_2O_3 transformation was evaluated.

Experimental procedures

The used raw powder is γ-Al_2O_3 transition alumina obtained by boehmite calcinations at 600 °C (boehmite being obtained by partial dehydration of gibbsite at 450 °C). The chemical composition expressed in weight % is given as follows: Al_2O_3(88.34%), SiO_2(3.86%), F(0.89%), Na_2O(0.34%), CaO_2(0.18%), Fe_2O_3(0.096%) and structural water(6%). The powder was attrition milled during 3 h using alumina balls of 2 mm diameter. A 0.25% mass ratio of DARVAN C as a dispersant and 1% of duramax as a bonder were added. During the milling process, the pH was adjusted at 10.4 [35]. After milling, the suspensions were completely dried at 110 °C. The powder was sieved to obtain aggregates smaller than 45 μm. In order to highlight the phase transformations, the thermal behaviour of the powder was studied using an analyser SETERAM TGA 92 allowing a differential thermal analysis (DTA). Thermal cycles were recorded from ambient up to 1600 °C with three heating rates (5, 10 and 20 °C/min). A powder mass of nearly 40 mg was used in all cases. The analysis by X-rays diffraction was carried out using Bruker D8 Advance diffractometer working at high temperatures. Green samples thermal shrinking was also studied between room temperature and 1300 °C. Dilatometry tests were carried out using a NETZSCHDIL402C dilatometer. The green compacts were initially shaped by uniaxial pressing then by cold isostatic pressing at 300 MPa. The samples were sintered at 1700 °C for 2 h. The final densities were determined by Archimedes's method using distilled water. The SEM micrographs were obtained using a JOEL 840A scanning electronic microscope. A 20 kV voltage and a working distance between 10 and 15 mm were used. The gold metalized polished surfaces were observed after a thermal treatment at 1600 °C during 1 h.

Please cite this article in press as: S. Lamouri, et al., Control of the γ-alumina to α-alumina phase transformation for an optimized alumina densification, Bol. Soc. Esp. Cerám. Vidr. (2016), http://dx.doi.org/10.1016/j.bsecv.2016.10.001

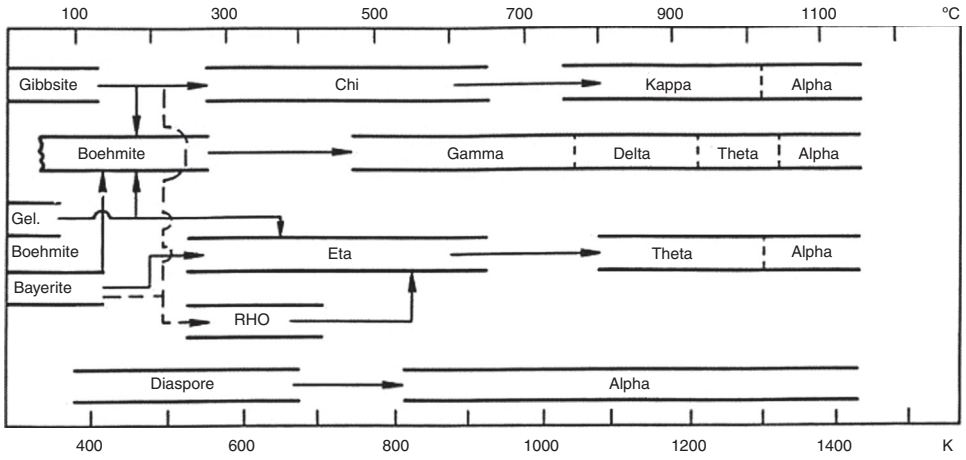

Fig. 1 – Transformation sequences of gibbsite ($Al(OH)_3$) to α-$A1_2O_3$ [10].

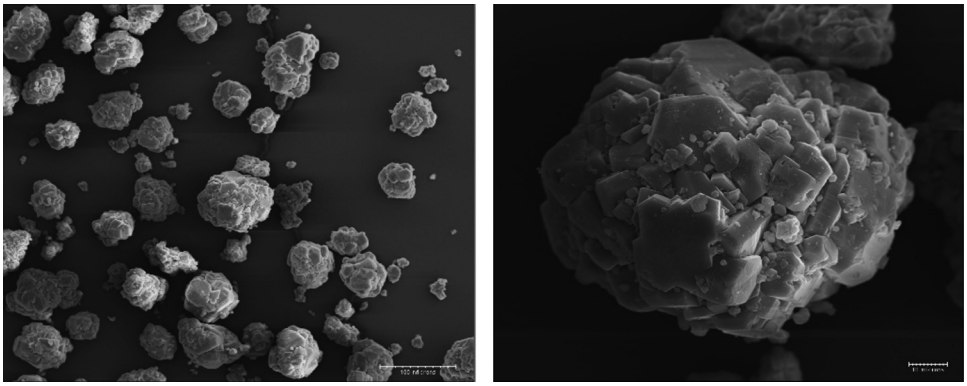

Fig. 2 – SEM micrographs of boehmite powder before milling.

Results and discussions

Raw powder

The morphology of the used raw boehmite is illustrated in Fig. 2. It consists of agglomerates of around 75 μm. The raw powder was attrition milled reducing its mean diameter (D_{50}) down to 0.29 μm (Fig. 3). The absolute density of the milled powder measured with helium pycnometer was 3.08 g/cm^3.

To obtain the γ-Al_2O_3 transition alumina phase, the milled boehmite was heated at 600 °C in order to completely eliminate the structural water according to established methods [30].

Differential thermal analysis

The thermal behaviour (DTA) of the γ-Al_2O_3 transition alumina powder, for different heating rates, is illustrated in Fig. 4.

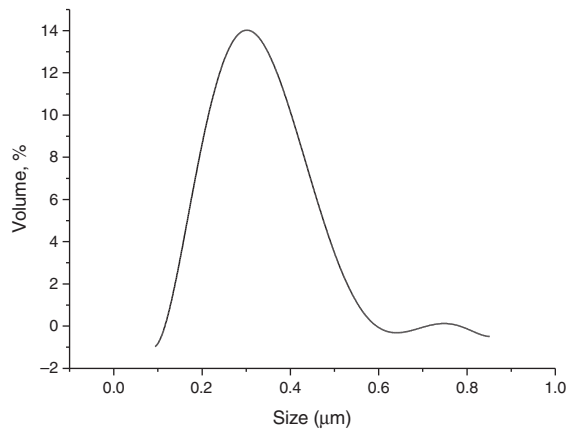

Fig. 3 – Particle size distribution for boehmite after 3 h attrition milling.

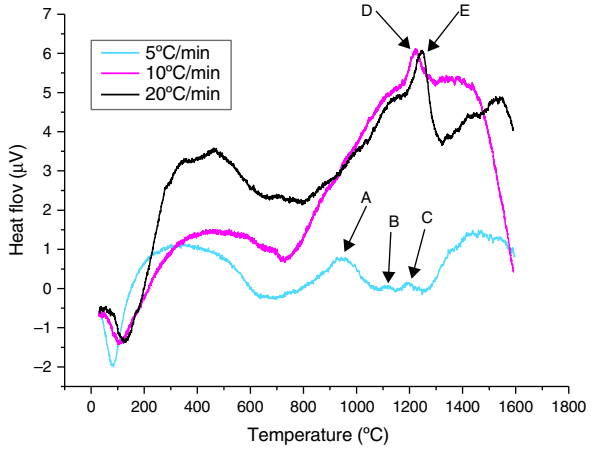

Fig. 4 – DTA curves of the γ-Al_2O_3 raw powder up to 1600 °C for different heating rates.

Please cite this article in press as: S. Lamouri, et al., Control of the γ-alumina to α-alumina phase transformation for an optimized alumina densification, Bol. Soc. Esp. Cerám. Vidr. (2016), http://dx.doi.org/10.1016/j.bsecv.2016.10.001

During the heating cycle between ambient and 1600 °C, the curves revealed that:

- For a 5 °C/min heating rate, the points A, B and C, three exothermic peaks of transition alumina transformation phases are observed. The first peak at around 800 °C is related to the transformation of γ-Al_2O_3 to the δ-Al_2O_3, the second at around 1080 °C is due to the δ-Al_2O_3 → θ-Al_2O_3 transformation and finally the third peak at 1150 °C to the θ-Al_2O_3 → α-Al_2O_3 phase transformation.
- For 10 and 20 °C/min heating rates, only the θ-Al_2O_3 → α-Al_2O_3 phase transformation appeared. They respectively start at 1217 °C (Point E) and 1240 °C (point F). Our results correspond to Weffer and Misra diagram [10]. A shift in the θ-Al_2O_3 → α-Al_2O_3 transformation peak for the three heating rates is also observed. The lowest heating rate reduces the temperature of α-Al_2O_3 formation. The transformation seems more progressive, with a larger and less intense peak than for higher heating rates.

Dilatometry

The shrinkage curves and their derivatives of the pressed samples are shown on (Fig. 5). They indicate two notable variations along the heating cycle. The samples shrinkage was disrupted by a small expansion indicating the θ-Al_2O_3 → α-Al_2O_3 phase transformation at 1056, 1082 and 1140 °C for the heating rate of 5, 10 and 20 °C/min respectively. The lowest heating rate promotes a maximum transformation rate at 1150 °C. This type of expansion was observed by different authors under the influence of alpha alumina doping seeds, sample compaction pressure rates and doping agents [8,34]. From the crystallographic point of view, the θ-Al_2O_3 → α-Al_2O_3 phase transformation occurs by crystallographic structure change (oxygen anion moving positions) from cubic face centred towards a compact hexagonal structure.

This transformation takes place by nucleation and growth mechanisms. It occurs with high activation energy depending on the heating rate [16–36]. In such transformation, the activation energy is mostly used in the nucleation process. This induces the temperatures shifts at the beginning of the θ-Al_2O_3 → α-Al_2O_3 phase transformation caused by the crystallographic reorganizations mechanisms [37]. In order to complete and evaluate the sintering process, a dilatometric cycle of γ-Al_2O_3 transition alumina of pressed green sample from ambient to 1700 °C with a 5 °C/min heating rate was made (Fig. 6). This test enables us to make a shrinkage process study. No volume variation was observed at the beginning of sintering process. This can be explained by the fact that the transition alumina phase transformations are characterized by structural changes without shrinkage. The θ-Al_2O_3 → α-Al_2O_3 phase transformation initiates at 1050 °C and reaches its maximum at 1192 °C.

DRX in situ

Fig. 7 shows the XRD patterns carried in situ from ambient to 1200 °C on boehmite attrition milled raw powder. The choice of this monohydrate comes from the fact that γ-Al_2O_3 transition alumina is produced from the dehydration of fine

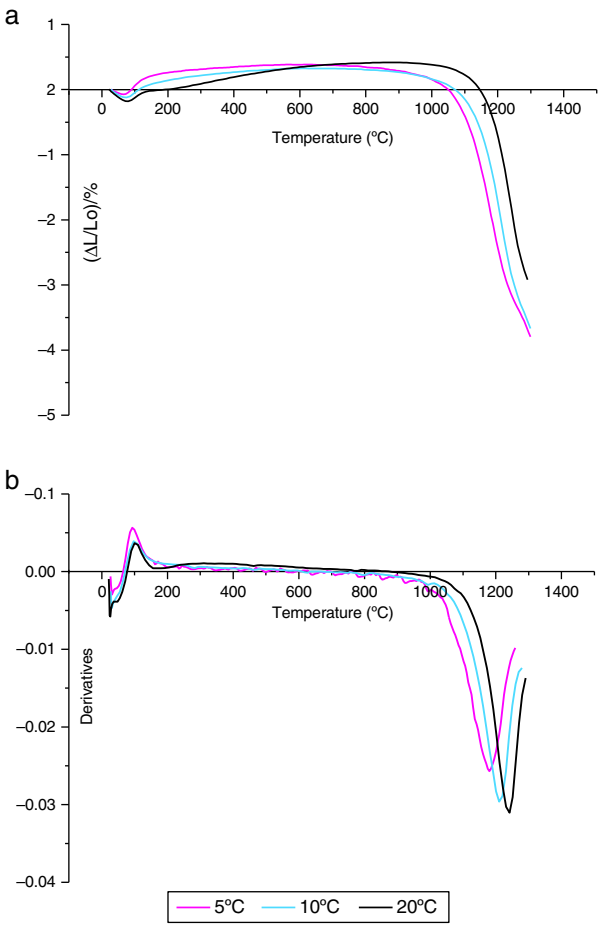

Fig. 5 – Dilatometry curves (a) and their derivatives (b) of the γ-Al_2O_3 transition alumina samples heated up to 1300 °C for different heating rates.

boehmite [10]. The XRD data were collected on a Bruker D8 Advance diffractometer with angular sweeping from 2θ = 42° until 2θ = 50° at 0.1°/min. The phases were identified by comparison with the JCPDS tables (γ-Al_2O_3: ICDD 50-741, δ-Al_2O_3: ICDD 16-394, θ-Al_2O_3: ICDD 23-1009, α-Al_2O_3: ICDD 46-1212). From the ambient to 450 °C, the diffractograms shows that the

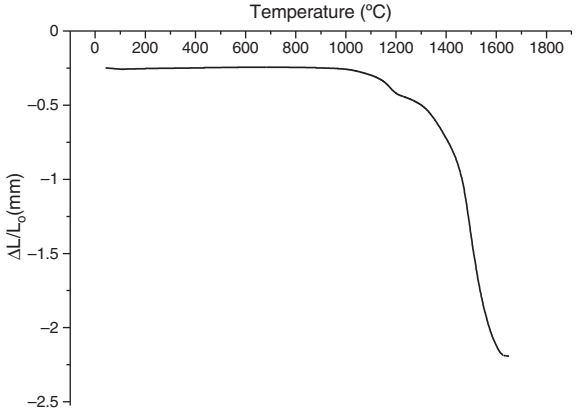

Fig. 6 – Dilatometry curve of the γ-Al_2O_3 transition alumina sample heated up to 1700 °C at 5 °C/min heating rate.

Please cite this article in press as: S. Lamouri, et al., Control of the γ-alumina to α-alumina phase transformation for an optimized alumina densification, Bol. Soc. Esp. Cerám. Vidr. (2016), http://dx.doi.org/10.1016/j.bsecv.2016.10.001

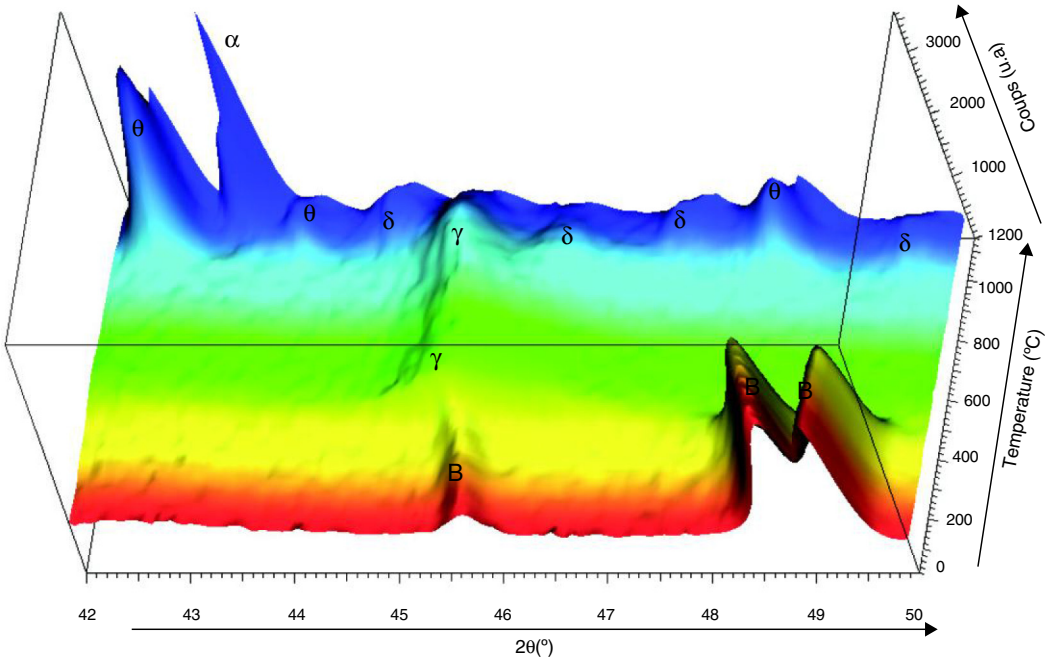

Fig. 7 – XRD in situ patterns of the raw boehmite attrition milled showing transformation from ambient to 1200 °C.

observed peaks correspond to crystalline boehmite. Boehmite is completely transformed to γ-Al_2O_3 in the temperature range 550 to 850 °C. The γ-Al_2O_3 and δ-Al_2O_3 phases coexist up to 950 °C. Beyond this temperature, the θ-Al_2O_3 starts to form progressively. The spectra of those "pseudo-amorphous" δ-Al_2O_3 and θ-Al_2O_3 phases decrease gradually with formation of the α-Al_2O_3 stable phase. Beyond 1200 °C, only the α-Al_2O_3 is observed.

Activation energy

Dilatometry and DTA tests were undertaken to evaluate the activation energy of θ-$Al_2O_3 \rightarrow$ α-Al_2O_3 transformation. The activation energy (E_a) values were obtained from transformation temperature peak measurements [20,38] using the three heating rates (Fig. 8). The activation energy values for θ-$Al_2O_3 \rightarrow$ α-Al_2O_3 transformation were estimated by Kissinger and (JMA) methods [39] using the following Eqs. (1) and (2), according to the peak temperature T_p at the different heating rates:

$$\ln\left(\frac{\phi}{T_p^2}\right) = -\frac{E_a}{RT_p} + \text{Cst} \quad (1)$$

$$\log[-\ln(1-x)] = -m\log\phi - \frac{1}{2.303}\frac{nE_a}{RT_p} + \text{Cst} \quad (2)$$

where 'ϕ' is the heating rate (K/s), T_p is the temperature corresponding to the maximum of θ → α-Al_2O_3 transformation peak (K), E_a is the activation energy of the θ → α-Al_2O_3 transformation (kJ/mol) and R is the ideal gas constant (8.314 J/mol K).

The relation characterizing the variable x:

$$x = \frac{A_T}{A_0},$$

Table 1 – Avrami parameter (n) values at different heating rates.

Heating rate (°C/min)	n	$t_{0.75}/t_{0.25}$
5	1.83	1.1.
10	2.25	1.08
20	2.73	1.05

where A_T is the area of the exothermic peak in the DTA curve at temperature T and A_0 is the area under the peak.

The plots obtained in Figs. 9 and 10, ($\ln(\phi/T_p^2)$ vs $1/T_p$) and ($\ln(\phi)$ vs $1/T_p$) respectively, are characterized by straight lines with different slopes E_a at different heating rates. The obtained activation energy value by dilatometry was about (464 kJ/mol). The one obtained by DTA is about 450 kJ/mol. These close values remain lower than those reported by Ma. Krell and Wang (517 kJ/mol) [38,39]. According to these results, the γ-Al_2O_3 transition alumina raw powder attrition milled contributes to lowering activation energy for the formation of the stable α alumina phase. On the other hand, the value of the exhibitor Avrami parameter [40,41], which reflects the transformation rate by germination and growth, is defined by (Eq. (3)) from the endothermic shape of crystallization obtained by DTA. The morphology of the crystal growth can be obtained at the transformation ratios (75% and 25%) [42].

$$n = \frac{2.5}{\Delta T}\frac{T_p^2}{E_a/R} \quad (3)$$

where ΔT is the width of the crystallization peak at half maximum value. The values of the Avrami constants are listed in Table 1. They increase from 1.83 to 2.73 with increasing heating rate. The average values of $t_{0.75}/t_{0.25}$ for each heating rate are also listed in Table 1. These values are very close suggesting

Please cite this article in press as: S. Lamouri, et al., Control of the γ-alumina to α-alumina phase transformation for an optimized alumina densification, Bol. Soc. Esp. Cerám. Vidr. (2016), http://dx.doi.org/10.1016/j.bsecv.2016.10.001

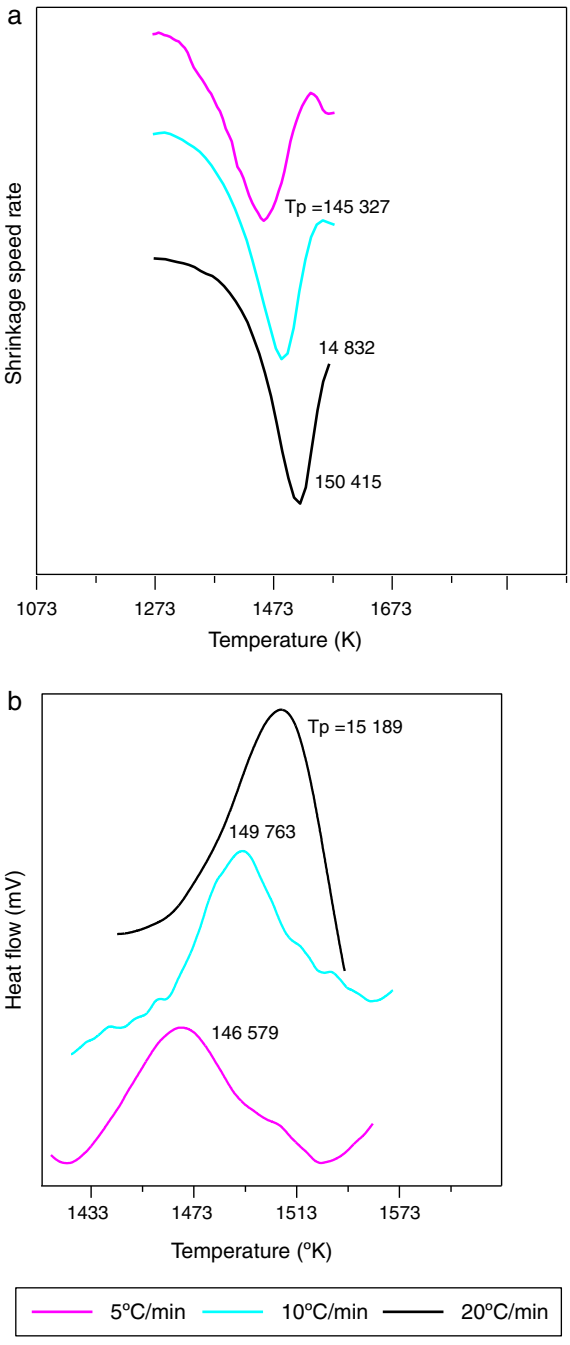

Fig. 8 – θ to α-Al_2O_3 maximum transformation peak of dilatometry derivative curves (a) and DTA curves (b) at various heating rates.

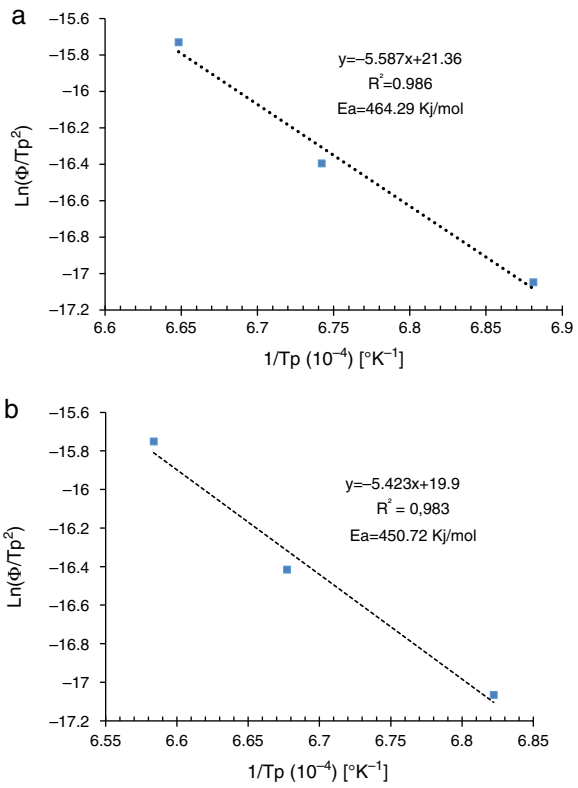

Fig. 9 – Plots of ln (Φ/T_p^2) versus $1/T_p$ (a) by dilatometry curves, (b) by DTA curves.

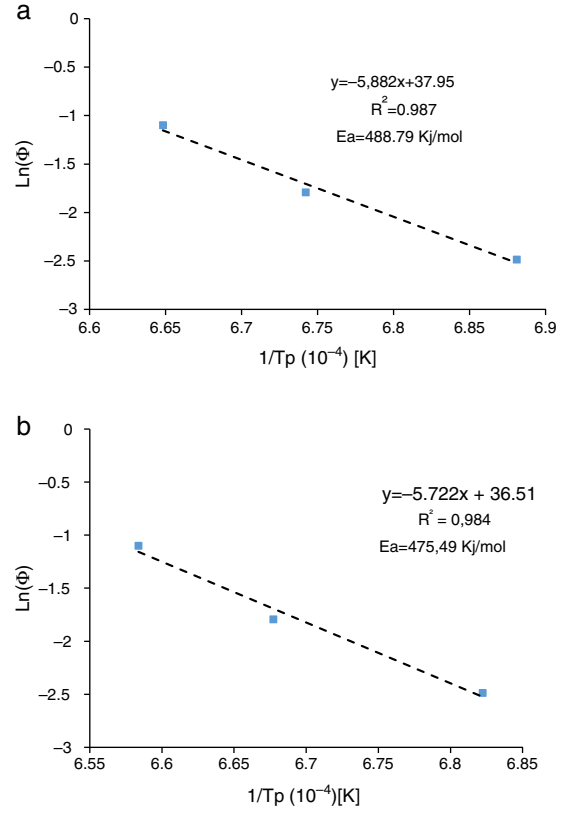

Fig. 10 – Plots of lnΦ versus $1/T_p$ (a) by dilatometry curves, (b) by DTA curves.

that the growth morphology is the same at the different heating rates.

Microstructure

The SEM micrographs of green bodies' sintered samples at 1700 °C are shown in Fig. 10. The γ-Al_2O_3 samples heated with a heating rate 20 °C/min had a porous structure with 85% of relative density and 1.6 μm grain mean size (Fig. 10a). For the sample fired with a 10 °C/min heating rate, a microstructure

Please cite this article in press as: S. Lamouri, et al., Control of the γ-alumina to α-alumina phase transformation for an optimized alumina densification, Bol. Soc. Esp. Cerám. Vidr. (2016), http://dx.doi.org/10.1016/j.bsecv.2016.10.001

improvement was noticed. The grain boundaries are quite apparent with important intergranular porosity. The relative density is 90% and the mean grains size is 1.54 μm (Fig. 10b). On the other hand, the samples heated at 5 °C/min had a dense and homogeneous microstructure with low residual porosity and 95% relative density and 3.2 μm mean grain size (Fig. 10c). The observed high density and homogeneous crystal structure with clearly apparent grain boundaries are a caused by a well established particles rearrangement during the θ-Al_2O_3 → α-Al_2O_3 transformation process (Fig. 11). The residual porosity in intra-granular parts was difficult to eliminate [19]. Otherwise,

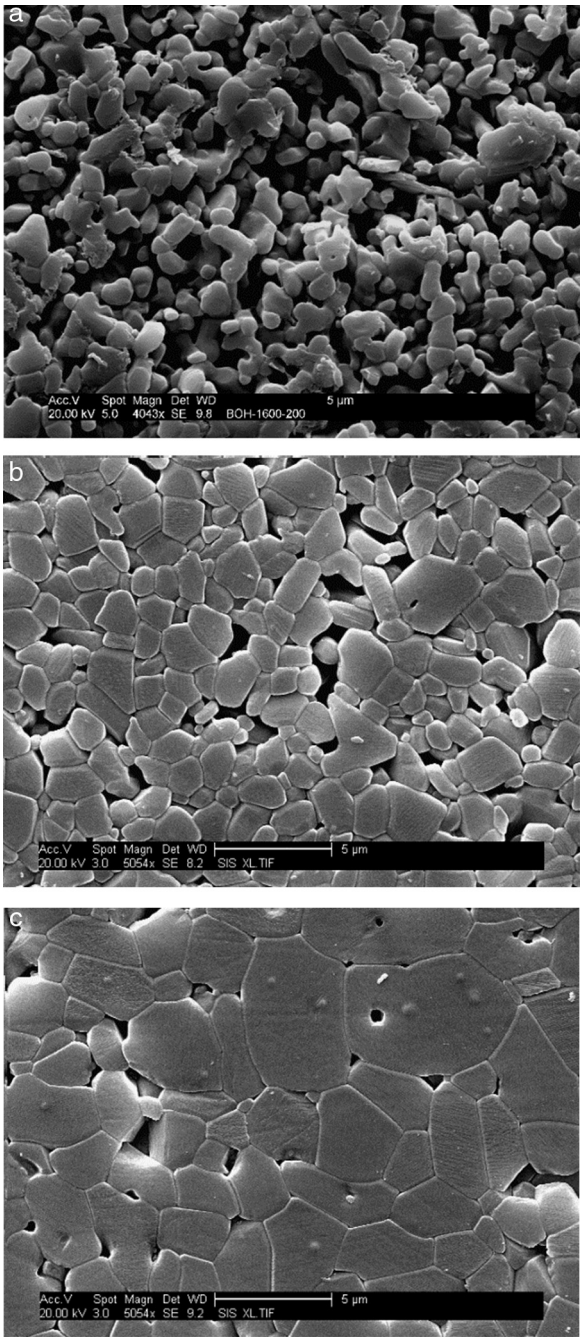

Fig. 11 – SEM images of γ-Al_2O_3 green bodies fired at 1700 °C with various heating rates: 20 °C/min (a), 10 °C/min (b), and 5 °C/min (c).

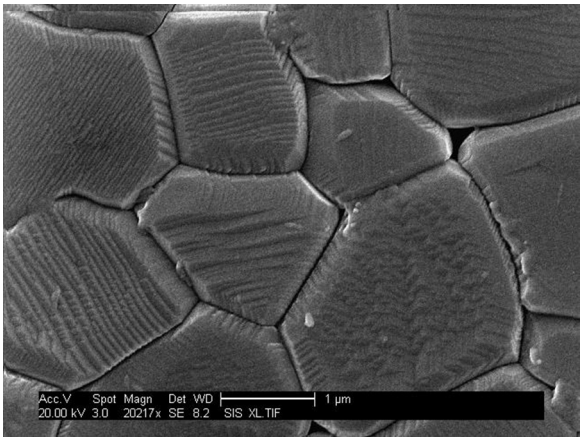

Fig. 12 – SEM images showing grains boundaries of γ-Al_2O_3 samples sintered at 1700 °C with 5 °C/min heating rate.

the presence of impurities in the starting alumina powder could be at the origin of liquid silicates formation. Generally, this glassy phase is located in grain boundaries and triple points. The formation of the amorphous phase facilitates alumina densification during sintering (Fig. 12).

Conclusion

The influence of the heating rate on the densification and microstructures of green bodies using γ-Al_2O_3 raw powder was studied during sintering. With a low heating rate (5 °C/min), the DTA curves showed a γ-Al_2O_3 → α-Al_2O_3 phase transformations. For higher heating rates (10 and 20 °C/min), only the θ-Al_2O_3 → α-Al_2O_3 phase transformation was detected. The dilatometry curves showed that the temperature at the beginning of the θ to α alumina transformation decreases with decreasing heating rates. The in situ XRD results for the boehmite raw powder used showed coexistence of different transition alumina during the phase transformations. The diffraction patterns in the temperature range (550–850 °C) correspond to the γ-Al_2O_3 phase. At 950 °C, this phase is still present and coexists with the δ-Al_2O_3 phase. Beyond this temperature, we observed the θ-Al_2O_3 → α-Al_2O_3 phase transformation. The activation energy for this transformation was evaluated using Kissinger equation from the results obtained by both DTA and dilatometry techniques. The SEM micrographs showed that samples heated at a 5 °C/min rate had a high relative density (95%) and homogeneous microstructure with low residual porosity.

REFERENCES

[1] L. Sedel, A. Raould, Engineering aspect of alumina on alumina hip prosthesis, in: Proc. Inst. Mech. Eng. II, J. Eng. Med. 221 (2007) 21–27.
[2] Z. Wang, D. Xue, X. Chen, B. Lu, H. Ratajezak, Mechanical and biomedical properties of hydroxyapatite-based gradient coating on α-Al_2O_3 ceramic substrate, J. Non-Cryst. Solids 351 (2005) 1675–1681.

Please cite this article in press as: S. Lamouri, et al., Control of the γ-alumina to α-alumina phase transformation for an optimized alumina densification, Bol. Soc. Esp. Cerám. Vidr. (2016), http://dx.doi.org/10.1016/j.bsecv.2016.10.001

[3] J.P. Ahn, J.K. Park, H.W. Lee, Effect of compact structures on the phase transition, subsequent densification and microstructure evolution during sintering of ultrafine gamma alumina powder, Nanostruct. Mater. 11 (1999) 133–140.
[4] G.C. Wei, Transparent ceramic lamp envelope materials, J. Phys. D: Appl. Phys. 38 (2005) 3057–3065.
[5] A. Krell, P. Blank, H. Ma, T. Hutzler, M.P.B. Van Brugyen, R. Apetz, Transparent sintered corundum with high hardness and strength, J. Am. Ceram. Soc. 86 (2003) 12–18.
[6] F.W. Dynys, J.W. Halloran, Influence of aggregates on sintering, J. Am. Ceram. Soc. 67 (1984) 596–601.
[7] J. Zheng, J.S. Reed, Effects of particle packing characteristics on solid-state sintering, J. Am. Ceram. Soc. 72 (1988) 810–817.
[8] C. Legros, C. Carry, P. Bowen, H. Hofmann, Sintering of a transition alumina: effects of phase transformation, powder characteristics and thermal cycle, J. Eur. Ceram. Soc. 19 (1999) 1967–1978.
[9] P. Bowen, C. Carry, D. Luxembourg, H. Hofmann, Colloidal processing and sintering of nanosized transition aluminas, Powder Technol. 157 (2005) 100–107.
[10] K. Wefers, C. Misra, Oxides and Hydroxides of Aluminium Alcoa Technical Paper N°19, Aluminium Company of America Pittsburgh, PA, 1987.
[11] Y. Yoshizawa, K. Hirao, S. Kazaki, Fabrication of low cost fine-grained alumina powders by seeding for high performance sintered bodies, J. Eur. Ceram. Soc. 24 (2004) 325–330.
[12] W.M. Zeng, L. Gao, J.K. Guo, A new sol–gel route using inorganic salt for synthesizing Al_2O_3 nanopowders, Nanostruct. Mater. 10 (1998) 543–550.
[13] J. Karthikeyan, C.C. Berndt, J. Tikkanen, S. Reddy, H. Herman, Plasma spray synthesis of nanomaterial powders and deposits, Mater. Sci. Eng. A 38 (1997) 275–286.
[14] O. Kiyoshi, H. Akiyoshi, T. Taketoshi, N. Akihiko, Effect of divalent cation additives on the γ-Al_2O_3 to α-Al_2O_3, phase transition, J. Am. Ceram. Soc. 83 (2000) 928–932.
[15] L. Pach, R. Roy, S. Komarneni, Nucleation of alpha alumina in boehmite gel, J. Mater. Res. 5 (1990) 278–285.
[16] F.W. Dynys, J.W. Halloran, Alpha alumina formation in alum-derived Gamma alumina, J. Am. Ceram. Soc. 65 (1982) 442–448.
[17] T.C. Chou, T.G. Nieh, Nucleation and concurrent anomalous grain growth of α-Al_2O_3 during γ-α phase transformation, J. Am. Ceram. Soc. 74 (1991) 2270–2279.
[18] T.C. Chou, T.G. Nieh, Interface-controlled phase transformation and abnormal grain growth of α-Al_2O_3 in thin γ-alumina films, Thin Solid Films 221 (1992) 89–97.
[19] K.B. Gan, C.I. Madsen, G.J. Hockridgea, In situ X-ray diffraction of the transformation of gibbsite to γ-alumina through calcination: effect of particle size and heating rate, J. Appl. Cryst. 42 (2009) 697–705.
[20] H. Belhouchet, M. Hamidouche, Bouaouadja, V. Garnier, G. Fantozzi, Crystallization kinetics of α-alumina and mullite-zirconia in boehmite and zircon mixture, J. Mater. Sci. Eng. A 3 (12) (2013) 814–819.
[21] P. Palmero, M. Lombardi, Effect of heating rate on phase and microstructural evolution, Int. J. Appl. Ceram. Technol. 6 (2009) 420–430.
[22] T. Hirayama, High-temperature characteristics of transition Al_2O_3 powder with ultrafine spherical particles, J. Am. Ceram. Soc. 7 (1987) C-122–C-124.
[23] P. Bowen, C. Carry, From powders to sintered pieces: forming, transformations and sintering of nanostructured ceramic oxides, Powder Technol. 128 (2002) 248–255.
[24] P.A. Badkar, J.E. Bailey, The mechanism of simultaneous sintering and phase transformation in alumina, J. Mater. Sci. 11 (1976) 1794–1806.
[25] F. Stenger, S. Mende, J. Schwedes, W. Peukert, The influence of suspension properties on the grinding behavior of alumina particles in the submicron size range in stirred media mills, Powder Technol. 156 (2005) 103–110.
[26] F. Stenger, S. Mende, W. Peukert, J. Schwedes, Mechanical production and stabilization of submicron particles in stirred media mills, Powder Technol. 132 (2003) 64–73.
[27] A. Tonejc, A.M. Tonejc, D. Bagović, C. Kosanović, Comparison of the transformation sequence from γ-AlOOH (boehmite) to α-Al_2O_3 (corundum) induced by heating and by ball milling, Mater. Sci. Eng. A 181–182 (1994) 1227–1231.
[28] M.L. Panchula, J.Y. Ying, Mechanical synthesis of nanocrystalline α-Al_2O_3 seeds for enhanced transformation kinetics, Nanostruct. Mater. 9 (1997) 161–164.
[29] S. Liu, L. Zhang, L. An, W. Fei, H. Heinrich, Phase transformation of mechanically milled nano-sized γ-alumina, J. Am. Ceram. Soc. 88 (2005) 2559–2563.
[30] P.S. Santos, H.S. Santos, S.P. Toledo, Standard transition aluminas. Electron microscopy studies, Mater. Res. 3 (2000) 104–114.
[31] A. Boumaza, L. Lavaro, J. Ledion, G. Satonnay, J.B. Brubach, P. Berthet, Transition alumina phases induced by heat treatment of boehmite: an X-ray diffraction and infrared spectroscopy study, Solid State Chem. 182 (2009) 1171–1176.
[32] C.S. Nordahl, G.L. Messing, Thermal analysis of phase transformation kinetics in α-Al_2O_3 seeded boehmite and γ-Al_2O_3, Thermochim. Acta 318 (1998) 187–199.
[33] Y. Yoshizawa, K. Hirao, S. Kanzaki, Fabrication of low cost fine grained alumina powders by seeding for high performance sintered bodies, J. Eur. Ceram. Soc. 24 (2004) 325–330.
[34] H. Belhouchet, M. Hamidouche, R. Torrecillas, G. Fantozzi, The non-isothermal kinetics of mullite formation in boehmite–zircon mixtures, J. Therm. Anal. Calorim. 116 (2014) 795–803.
[35] H. Belhouchet, M. Hamidouche, Bouaouadja, V. Garnier, G. Fantozzi, Elaboration and microstrutural characterization of a mullite-zirconia composite obtained by reaction sintering, Ann. Chim. Sci. Mater. 32 (2007) 605–614.
[36] S. Wu, L.C. De Jonghe, Sintering of nanophase gamma-Al_2O_3 powder, J. Am. Ceram. Soc. 79 (1996) 2207–2211.
[37] R.S. Mishra, C.E. Lesher, A.K. Mukherjee, High-pressure sintering of nanocrystalline γ-Al_2O_3, J. Am. Ceram. Soc. 79 (1996) 2989–2992.
[38] H. Ma, A. Krell, Synthesis and processing of nano-α-Al_2O_3 powders, Key Eng. Mater. 206–213 (2002) 43–46.
[39] H.E. Kissinger, Variation of peak temperature with heating rate in differential thermal analysis, J. Res. Nation. Bur. Stand. 57 (1956) 217–221.
[40] H.G. Wang, H. Herman, X. Liu, Activation energy for crystal growth using isothermal and continuous heating processes, J. Mater. Sci. 25 (1990) 2339–2343.
[41] J.A. Augis, J.D. Bennet, Calculation of Avrami parameters for heterogeneous solid-state reactions using a modification of Kissinger method, J. Therm. Anal. Cal. 13 (1978) 283–292.
[42] A.K. Jena, M.C. Chaturvedi, Phase Transformations in Materials, Prentice Hall, Englewood Cliffs, NJ, 1992, pp. 247.

Please cite this article in press as: S. Lamouri, et al., Control of the γ-alumina to α-alumina phase transformation for an optimized alumina densification, Bol. Soc. Esp. Cerám. Vidr. (2016), http://dx.doi.org/10.1016/j.bsecv.2016.10.001